Infectious Disease Modelling 3 (2018) 35–59

Contents lists available at ScienceDirect

Infectious Disease Modelling

journal homepage: www.keaipublishing.com/idm

Transmission dynamics and control strategies assessment of avian influenza A (H5N6) in the Philippines

Hanl Lee [a], Angelyn Lao [a, b, *]

[a] Mathematics & Statistics Department, De La Salle University, 2401 Taft Avenue, 0922 Manila, Philippines
[b] Mathematical & Statistical Modeling Research Unit, Center for Natural Sciences and Environmental Research, 2401 Taft Avenue, 0922 Manila, Philippines

ARTICLE INFO

Article history:
Received 18 December 2017
Received in revised form 21 February 2018
Accepted 8 March 2018
Available online 16 March 2018
Handling Editor: Jianhong Wu

Keywords:
Avian influenza
Half-saturated incidence
Personal protection
Isolation
Vaccination
Philippines

ABSTRACT

Due to the outbreaks of Highly Pathogenic Avian Influenza A (HPAI) H5N6 in the Philippines (particularly in Pampanga and Nueva Ecija) in August 2017, there has been an increase in the need to cull the domestic birds to control the spread of the infection. However, this control method poses a negative impact on the poultry industry. In addition, the pathogenicity and transmissibility of the H5N6 in both the birds and the humans remain largely unknown which call for the necessity to develop more strategic control methods for the virus. In this study, we constructed a mathematical model for the bilinear and half-saturated incidence to compare their corresponding effect on transmission dynamics of H5N6. The simulations of half-saturated incidence model were similar to what occurred during the H5N6 outbreak (2017) in the Philippines. Instead of culling the birds, we implemented other control strategies such as non-medicinal (personal protection and poultry isolation) and medicinal (poultry vaccination) ways to prevent, reduce, and control the rate of the H5N6 virus transmission. Among the proposed control strategies, we have shown that the poultry isolation strategy is still the most effective in reducing the infected birds.

1. Introduction

H5N6, a subtype of avian influenza A, is a virus that mutated from H5N1 - another type of avian influenza virus that is as highly pathogenic as H5N6 (since 2003) (Analysis, 2016). The highly pathogenic H5N6, which is easily visible among the population of the birds, is considered to be the most recent avian influenza that started to appear in China since May 2014 (Joob & Viroj, 2015). In the past, lowly pathogenic avian influenza H5N6 had already occurred in several areas of the world such as Germany (1984), Sweden (2002), and the U.S.A (1975, 2013), but the effects on the poultry industry and public health were trivial. In contrast to the preceding events, the HPAI H5N6 that arose in China (2014) critically infected and killed the birds and humans (Claes & Von Dobschuetz, 2014).

* Corresponding author. Mathematics & Statistics Department, De La Salle University, 2401 Taft Avenue, 0922 Manila, Philippines.
E-mail addresses: hanl_lee@dlsu.edu.ph (H. Lee), angelyn.lao@dlsu.edu.ph (A. Lao).
Peer review under responsibility of KeAi Communications Co., Ltd.

https://doi.org/10.1016/j.idm.2018.03.004

Studies have revealed that all cases of H5N6 in humans have contact with live poultry or live poultry markets. Although the risk of this disease transmission from poultry to humans is measured to be low, there have been 16 cases in which the H5N6 severely infected the humans and six cases that caused deaths from China (WPRO). Among the 16 cases, 11 patients were reported to be infected with the deadly virus which resulted to a case fatality rate of 69% (World Health Organization, 2017). The symptoms of H5N6 in humans may include fever, diarrhea, pneumonia, multi-organ failure, encephalitis, septic shock, and conjunctivitis (HPAI, 2015).

The first outbreak of HPAI H5N6 in the Philippines occurred in July 24, 2017 in San Luis, Pampanga and two subsequent incidents also happened in Jaen and San Isidro, Nueva Ecija. In the latter part of August 2017, test results confirmed the strain to be positive for H5N6 (OIE). Even though the source of H5N6 transmission still remains to be unknown, the Department of Agriculture suspected that the reason of transmission was either by the migrant birds or the Peking ducks which were illegally traded (Negative for H5N1). No cases of human infections and deaths due to H5N6 occurred whatsoever but a total of 45,682 birds died while 393,515 birds were killed and disposed of (OIE). As a result, the incidents had a critical damage on the poultry industry with an estimated daily loss of 179 million pesos (Avian flu poultry ban partially lifted). Instead of culling the birds, control strategies that may control and prevent the spread of avian influenza ought to be taken into consideration (Bowman, Gumel, van den Driessche, Wu, & Zhu, 2005).

Mathematical modeling studies regarding the H5N6 are rarely found but there are a number of papers that model other strains of avian influenza for birds and human populations (Chong, Tchuenche, & Smith, 2014; Liu & Fang, 2015; Liu, Pang, Ruan, & Zhang, 2015). For simplicity, several studies preferred to use bilinear incidence models in investigating the transmission of avian influenza in both bird and human population (Brauer & Castillo-Chavez, 2012; Buonomo & Lacitignola, 2008; Liu & Fang, 2015). However, in order to achieve the significant decrease in the population of infected humans, recent models in relation to avian influenza have started to consider saturated incidence instead of bilinear incidence (Chong et al., 2014; Gao, Chen, Nieto, & Torres, 2006; Yang, Zhang, & Wang, 2017). In the papers by Liu, Ruan, & Zhang (2015, 2017) and Zhang et al. (2017), they modeled the spread of H7N9 using both semilinear and half-saturated incidence rates.

In the studies done by Chong et al. (2014) and Liu, Pang, et al. (2015), models that consider saturation incidence rate to investigate the effect on transmission dynamics of the avian influenza were both established. Chong et al. examined the effect of pharmaceutical and non-pharmaceutical control strategies, whereas Liu et al. considered the psychological effect on humans in response to the outbreaks of avian influenza.

To study the dynamics of the HPAI H5N6 outbreaks in the Philippines, we built an extension of the mathematical models done by Chong et al. and Liu et al. With the modified model described in Section 2, we performed stability analysis of the avian-only and avian-human model on the basis of bilinear incidence (shown in Section 3) and half-saturated incidence (shown in Section 4).

In Section 5, comparison between the effect of bilinear incidence and half-saturated incidence on infected individuals is done. Whereas, case studies on endemic condition with different control strategies that will prevent or reduce the transmission of H5N6 are examined in Section 6. The control strategies that are considered in our model include endemic case, personal protection for humans, isolation for birds, and vaccination for birds which will be useful in controlling the transmission of the avian influenza and may also be practical in investigating other diseases such as similar strains of H5N6. In the end, we hope to determine which control strategy proves to be the most effective in preventing and controlling the spread of avian influenza.

2. Materials and methodology

In the schematic diagram, shown in Fig. 1, we have two hosts: bird population ($N_b(t)$) and human population ($N_h(t)$) where $N_b = S_b + I_b$ and $N_h = S_h + I_a$. In the bird population (shown at the upper portion of Fig. 1), the susceptible birds S_b and infected birds I_b are present. The inflow Λ_b in S_b represents an increase due to the birth rate of the birds while the outflow

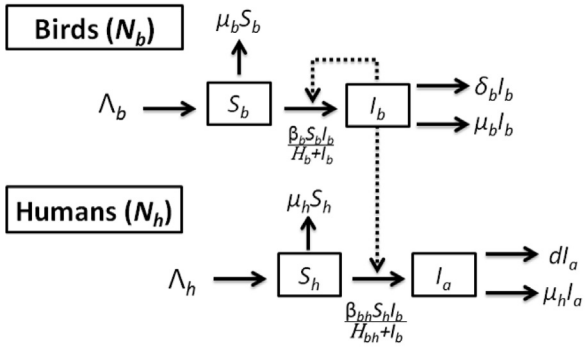

Fig. 1. The two-host model of H5N6 virus transmission in birds and humans.

$\mu_b S_b$ indicates a decrease in the bird population due to natural death. Another outflow in S_b (represented by $\frac{\beta_b S_b I_b}{H_b+I_b}$) describes a reduction in the susceptible bird population due to the avian influenza disease transmitted through direct contact with infected birds.

In turn, $\frac{\beta_b S_b I_b}{H_b+I_b}$ becomes an inflow of I_b since the infected birds are no longer susceptible. The outflow $\delta_b I_b$ and $\mu_b I_b$ of I_b symbolize the decrease in infected bird population due to death by avian influenza strain in birds and natural death, respectively. The dashed directional arrow from I_b to the transition between S_b and I_b is indicated in such a way that $\frac{\beta_b S_b I_b}{H_b+I_b}$ is regulated by I_b. The transition from I_b to the conversion from S_h to I_a has the same basis as well.

Similarly, in the human population (shown at the lower portion of Fig. 1), the population of susceptible humans S_h is increased by the birth rate Λ_h but is reduced due to natural death $\mu_h S_h$ and from the H5N6 disease contracted from the infected birds (represented by $\frac{\beta_{bh} S_h I_b}{H_{bh}+I_b}$). Simultaneously, $\frac{\beta_{bh} S_h I_b}{H_{bh}+I_b}$ expands the population of infected humans with avian strain I_a and two factors such as natural death $\mu_h I_a$ and death caused by avian strain in humans dI_a decrease I_a.

The definitions and symbols of the model variables are specified in Table 1 while the value of the parameters (either taken from existing literature or estimated) are listed in Appendix B Table 3.

Considering the interactions of birds and humans, as illustrated in Fig. 1, we built the avian influenza models, both the bilinear (Section 3) and the half-saturated incidence (Section 4).

3. Avian-human bilinear incidence (BI) model

To examine the difference between the half-saturated incidence model and the bilinear, we first build the avian influenza model with bilinear incidence (i.e. the susceptible individuals having equal probability of contracting the disease where bilinear incidence rate is expressed as βSI (Chong et al., 2014)) as shown below:

$$S_b'(t) = \Lambda_b - \mu_b S_b - \beta_b S_b I_b \tag{1}$$

$$I_b'(t) = \beta_b S_b I_b - (\mu_b + \delta_b) I_b \tag{2}$$

Table 1
List of model variables and parameters with definitions.

Symbol	Definition
$S_b(t)$	Susceptible birds
$I_b(t)$	Infected birds
$S_h(t)$	Susceptible humans
$I_a(t)$	Infected humans with avian strain
$V_b(t)$	Vaccinated birds
$T_b(t)$	Isolated birds
$R_b(t)$	Recovered birds from avian strain
$N_b(t)$	Total bird population
$N_h(t)$	Total human population
Λ_b	Bird inflow
Λ_h	Human inflow
μ_b	Natural death rate of birds
μ_h	Natural death rate of humans
β_{bh}	Rate at which bird-to-human avian influenza is contracted
β_b	Rate at which birds contract avian influenza
β_v	Rate at which vaccinated birds contract avian influenza
H_b	Half-saturation constant for birds with avian strain
H_{bh}	Half-saturation constant for humans with avian strain from infected birds
H_v	Half-saturation constant for vaccinated birds with avian strain
d	Additional disease death rate due to avian strain in humans
δ_b	Additional disease death rate due to avian strain in birds
p	Prevalence rate of the vaccination program
ϕ	Efficacy of the vaccine
γ_b	Recovery rate of birds with avian strain
c	Percentage of the population employing personal protection
q	Efficiency of personal protection
$S_b(0)$	Susceptible birds at $t = 0$
$I_b(0)$	Infected birds at $t = 0$
$S_h(0)$	Susceptible humans at $t = 0$
$I_a(0)$	Infected humans with avian strain at $t = 0$
$V_b(0)$	Vaccinated birds at $t = 0$
$T_b(0)$	Isolated birds at $t = 0$
$R_b(0)$	Recovered birds from avian strain at $t = 0$

$$S_h'(t) = \Lambda_h - \mu_h S_h - \beta_{bh} S_h I_b \tag{3}$$

$$I_a'(t) = \beta_{bh} S_h I_b - (\mu_h + d) I_a \tag{4}$$

The terms having positive signs represent enlargement whereas, the terms having negative signs indicate reduction with respect to the associated variable (see Table 1 for the description of the parameters).

3.1. Stability analysis of the avian-only BI model

Given the bilinear incidence model of the avian influenza, we perform stability analysis to determine whether the basic reproduction number R_0 of the calculated disease-free equilibrium (DFE) is locally asymptotically stable or not. In the *avian-only BI model*, we considered the first two equations of bilinear incidence model only (i.e. Equations (1) and (2)) to obtain the DFE of the birds.

3.1.1. Disease-free equilibrium, E_B^0

By disease-free, we mean the absence of infection among the birds which makes $I_b = 0$. To solve for the number of susceptible birds at the DFE state (denoted by S_b^0), we let $S_b'(t) = 0$ in Equation (1):

$$\begin{aligned} S_b'(t) &= \Lambda_b - \mu_b S_b - \beta_b S_b I_b \\ 0 &= \Lambda_b - \mu_b S_b \\ S_b^0 &= \frac{\Lambda_b}{\mu_b}. \end{aligned}$$

We have shown that the DFE of the *avian-only BI model* is represented by

$$E_B^0 = \left(S_b^0, I_b^0\right) = \left(\frac{\Lambda_b}{\mu_b}, 0\right). \tag{5}$$

3.1.2. Endemic equilibrium, E_B^*

In an endemic equilibrium (EE) state, the avian flu spreads rapidly among the bird population within a short span of time. Hence, in this state, the number of infected birds $I_b \neq 0$. To obtain the number of susceptible birds S_b^* at the EE state, we let $I_b'(t) = 0$ in Equation (2):

$$\begin{aligned} I_b'(t) &= \beta_b S_b I_b - (\mu_b + \delta_b) I_b \\ 0 &= \beta_b S_b I_b - (\mu_b + \delta_b) I_b \\ S_b^* &= \frac{\mu_b + \delta_b}{\beta_b}. \end{aligned} \tag{6}$$

To solve for I_b^*, we let $S_b'(t) = 0$ in Equation (1):

$$\begin{aligned} S_b'(t) &= \Lambda_b - \mu_b S_b - \beta_b S_b I_b \\ 0 &= \Lambda_b - \mu_b S_b - \beta_b S_b I_b \\ S_b &= \frac{\Lambda_b}{\mu_b + \beta_b I_b}. \end{aligned} \tag{7}$$

Substituting Equation (6) into Equation (7),

$$\begin{aligned} \frac{\Lambda_b}{\mu_b + \beta_b I_b} &= \frac{\mu_b + \delta_b}{\beta_b} \\ I_b^* &= \frac{\Lambda_b \beta_b - \mu_b(\mu_b + \delta_b)}{\beta_b(\mu_b + \delta_b)}. \end{aligned} \tag{8}$$

Thus, the EE of the *avian-only BI model* is represented by

$$E_B^* = (S_b^*, I_b^*) = \left(\frac{\mu_b + \delta_b}{\beta_b}, \frac{\Lambda_b\beta_b - \mu_b(\mu_b + \delta_b)}{\beta_b(\mu_b + \delta_b)}\right). \tag{9}$$

3.1.3. Basic reproduction number, R_B

Next, we generate the basic reproduction number (see Appendix A.1 for further discussion) R_B for DFE state of the *avian-only BI model*. We take the rate at which the susceptible birds contract the flu (denoted by $\beta_b S_b I_b$). Letting $\bar{x} = [I_b(t)]$, $F_i(\bar{x}) = [\beta_b S_b I_b]$. We let the transmission of the susceptible class into the infectious class (denoted by **F**, where the (i,j) entry of **F** represents the rate at which infected individuals in class j generates new infections in class i (Van den Driessche & Watmough, 2002).) be defined by

$$\begin{aligned}\mathbf{F} &= \left[\frac{\partial(\beta_b S_b I_b)}{\partial I_b}\right] \\ &= [\,\beta_b S_b\,].\end{aligned} \tag{10}$$

Substituting DFE in (5) into matrix **F** in (10),

$$\mathbf{F}\left(E_B^0\right) = \frac{\beta_b \Lambda_b}{\mu_b}.$$

Aside from the transmission matrix **F**, we also need to consider the transition matrix **V**, which corresponds to the population that are transferred into and out from the infectious class I_b. For the population transferred into the infectious class, the susceptible class is excluded. This gives us

$$V_i(\bar{x}) = V_i^-(\bar{x}) - V_i^+(\bar{x}) = (\mu_b + \delta_b)I_b - 0 = (\mu_b + \delta_b)I_b$$

such that

$$\mathbf{V} = \left[\frac{\partial(\mu_b + \delta_b)I_b}{\partial I_b}\right] = [\,\mu_b + \delta_b\,]$$

and

$$\mathbf{V}^{-1} = \frac{1}{\mu_b + \delta_b},$$

where the $(j,\ k)$ entry of $\mathbf{V}^{-1}$ is expressed as the expected period of time such that an individual remains in class j (Van den Driessche & Watmough, 2002).

Therefore, the basic reproduction number for DFE state of the *avian-only BI model* is

$$R_B = \mathbf{F}\mathbf{V}^{-1}\left(E_B^0\right) = \frac{\beta_b \Lambda_b}{\mu_b(\mu_b + \delta_b)}. \tag{11}$$

When the parameters $\beta_b = \frac{45{,}685}{439{,}197\times 30}$, $\Lambda_b = \frac{2{,}060}{365}$, $\mu_b = \frac{1}{2\times 365}$, and $\delta_b = \frac{45{,}682}{439{,}197\times 30}$ from Table 3, the basic reproduction number in (11) is

$$R_B = 2953.3764. \tag{12}$$

We now determine if the DFE E_B^0 of *avian-only BI model* is locally asymptotically stable or not with the following theorem.

Theorem 3.1. (Stability of the DFE (Castillo-Chavez & Song, 2004; Van den Driessche & Watmough, 2002)). *The disease-free equilibrium E^0 is*

1. *Locally asymptotically stable, if $R_0 \leq 1$ (disease dies off).*
2. *Locally asymptotically unstable, if $R_0 > 1$ (disease persists).*

By Theorem 3.1, E_B^0 is locally asymptotically unstable, which suggests that this model has an endemic equilibrium.

3.2. Stability analysis of the avian-human BI model

In this section, we take the interaction between the population of the birds and humans into consideration and consider Equations (1)–(4) of the BI model. Similarly to what we did for the avian-only BI model, we derive the basic reproduction number for the disease-free state of the *avian-human BI model*.

3.2.1. Disease-free equilibrium, E^0_{AH}

Since the infection among the birds under the DFE state does not exist and does not affect humans, the number of humans with avian strain $I_a = 0$. To solve for the number of susceptible humans at the DFE state (denoted by S^0_h), we let ${S_h}'(t) = 0$ in Equation (3):

$$\begin{aligned} {S_h}'(t) &= \Lambda_h - \mu_h S_h \\ 0 &= \Lambda_h - \mu_h S_h \\ S^0_h &= \frac{\Lambda_h}{\mu_h}. \end{aligned}$$

Thereby, the DFE of the *avian-human BI model* is represented by

$$E^0_{AH} = \left(S^0_b, I^0_b, S^0_h, I^0_a\right) = \left(\frac{\Lambda_b}{\mu_b}, 0, \frac{\Lambda_h}{\mu_h}, 0\right). \tag{13}$$

3.2.2. Endemic equilibrium, E^*_{AH}

In an EE state, since the infection among the birds exists and is capable of infecting the humans, the number of humans with avian strain $I_a \neq 0$. To solve for the number of susceptible humans at the EE state, S^*_h, we let ${S_h}'(t) = 0$ in Equation (3):

$$\begin{aligned} {S_h}'(t) &= \Lambda_h - \mu_h S_h - \beta_{bh} S_h I_b \\ 0 &= \Lambda_h - \mu_h S_h - \beta_{bh} S_h I_b \\ S_h &= \frac{\Lambda_h}{\mu_h + \beta_{bh} I_b}. \end{aligned} \tag{14}$$

Substituting $I^*_b = \frac{\Lambda_b \beta_b - \mu_b(\mu_b + \delta_b)}{\beta_b(\mu_b + \delta_b)}$ (shown in Equation (8)) into Equation (14),

$$\begin{aligned} S_h &= \frac{\Lambda_h}{\mu_h + \beta_{bh} I_b} \\ S^*_h &= \frac{\Lambda_h \beta_b(\mu_b + \delta_b)}{\mu_h \beta_b(\mu_b + \delta_b) + \beta_{bh}[\Lambda_b \beta_b - \mu_b(\mu_b + \delta_b)]}. \end{aligned}$$

To solve for the number of infected humans with avian strain at EE state, I^*_a, we let ${I_a}'(t) = 0$ in Equation (4):

$$\begin{aligned} {I_a}'(t) &= \beta_{bh} S_h I_b - (\mu_h + d) I_a \\ 0 &= \beta_{bh} S_h I_b - (\mu_h + d) I_a \\ S_h &= \frac{(\mu_h + d) I_a}{\beta_{bh} I_b}. \end{aligned} \tag{15}$$

Substituting Equation (14) into Equation (15),

$$\begin{aligned} \frac{\Lambda_h}{\mu_h + \beta_{bh} I_b} &= \frac{(\mu_h + d) I_a}{\beta_{bh} I_b} \\ I_a &= \frac{\Lambda_h \beta_{bh} I_b}{(\mu_h + d)(\mu_h + \beta_{bh} I_b)}. \end{aligned} \tag{16}$$

Substituting $I^*_b = \frac{\Lambda_b \beta_b - \mu_b(\mu_b + \delta_b)}{\beta_b(\mu_b + \delta_b)}$ (shown in Equation (8) into Equation (16),

$$I_a = \frac{\Lambda_h \beta_{bh}\left[\frac{\Lambda_b\beta_b - \mu_b(\mu_b+\delta_b)}{\beta_b(\mu_b+\delta_b)}\right]}{(\mu_h+d)\left[\left(\mu_h + \beta_{bh}\left(\frac{\Lambda_b\beta_b - \mu_b(\mu_b+\delta_b)}{\beta_b(\mu_b+\delta_b)}\right)\right)\right]}$$
$$I_a^* = \frac{\Lambda_h\beta_{bh}[\Lambda_b\beta_b - \mu_b(\mu_b+\delta_b)]}{(\mu_h+d)[\mu_h\beta_b(\mu_b+\delta_b) + \beta_{bh}(\Lambda_b\beta_b - \mu_b(\mu_b+\delta_b))]}. \tag{17}$$

Hence, the EE of the *avian-human BI model* is represented by

$$\begin{aligned} E_{AH}^* &= (S_b^*, I_b^*, S_h^*, I_a^*) \\ &= \left(\frac{\mu_b+\delta_b}{\beta_b}, \frac{\Lambda_b\beta_b - \mu_b(\mu_b+\delta_b)}{\beta_b(\mu_b+\delta_b)}, \right. \\ &\quad \frac{\Lambda_h\beta_b(\mu_b+\delta_b)}{\mu_h\beta_b(\mu_b+\delta_b) + \beta_{bh}[\Lambda_b\beta_b - \mu_b(\mu_b+\delta_b)]}, \\ &\quad \left. \frac{\Lambda_h\beta_{bh}[\Lambda_b\beta_b - \mu_b(\mu_b+\delta_b)]}{(\mu_h+d)[\mu_h\beta_b(\mu_b+\delta_b) + \beta_{bh}(\Lambda_b\beta_b - \mu_b(\mu_b+\delta_b))]}\right). \end{aligned} \tag{18}$$

3.2.3. Basic reproduction number, R_{AH}

Given the two infectious classes, I_b and I_a, the dimension of the transmission matrix $\mathbf{F}$ is 2×2. For I_a, the new rate at which the susceptible humans contract the avian flu carried by the bird is $\beta_{bh}S_hI_b$. Letting $\overline{x} = [I_b(t), I_a(t)]^T$,

$$F_i(\overline{x}) = \begin{bmatrix} \beta_b S_b I_b \\ \beta_{bh} S_h I_b \end{bmatrix}$$

such that

$$\mathbf{F} = \begin{bmatrix} \beta_b S_b & 0 \\ \beta_{bh} S_h & 0 \end{bmatrix}. \tag{19}$$

Substituting DFE in (13) into matrix $\mathbf{F}$ in (19),

$$\mathbf{F}\left(E_{AH}^0\right) = \begin{bmatrix} \frac{\beta_b\Lambda_b}{\mu_b} & 0 \\ \frac{\beta_{bh}\Lambda_h}{\mu_h} & 0 \end{bmatrix}.$$

Whereas, the transition matrix $\mathbf{V}$ with respect to I_b and I_a is given by

$$\begin{aligned} V_i(\overline{x}) &= V_i^-(\overline{x}) - V_i^+(\overline{x}) \\ &= \begin{bmatrix} (\mu_b+\delta_b)I_b \\ (\mu_h+d)I_a \end{bmatrix} - \begin{bmatrix} 0 \\ 0 \end{bmatrix} \\ &= \begin{bmatrix} (\mu_b+\delta_b)I_b \\ (\mu_h+d)I_a \end{bmatrix} \end{aligned}$$

such that

$$\mathbf{V} = \begin{bmatrix} \mu_b+\delta_b & 0 \\ 0 & \mu_h+d \end{bmatrix}$$

and

$$\mathbf{V}^{-1} = \frac{1}{(\mu_b+\delta_b)(\mu_h+d)}\begin{bmatrix}\mu_h+d & 0\\ 0 & \mu_b+\delta_b\end{bmatrix} = \begin{bmatrix}\frac{1}{\mu_b+\delta_b} & 0\\ 0 & \frac{1}{\mu_h+d}\end{bmatrix}.$$

Consequently,

$$\mathbf{FV}^{-1}\left(E^0_{AH}\right) = \begin{bmatrix}\frac{\beta_b\Lambda_b}{\mu_b} & 0\\ \frac{\beta_{bh}\Lambda_h}{\mu_h} & 0\end{bmatrix}\begin{bmatrix}\frac{1}{\mu_b+\delta_b} & 0\\ 0 & \frac{1}{\mu_h+d}\end{bmatrix} = \begin{bmatrix}\frac{\beta_b\Lambda_b}{\mu_b(\mu_b+\delta_b)} & 0\\ \frac{\beta_{bh}\Lambda_h}{\mu_h(\mu_b+\delta_b)} & 0\end{bmatrix}.$$

To get the eigenvalues $(\lambda_\pm)$ of $\mathbf{FV}^{-1}(E^0_{AH})$ with trace $T = \frac{\beta_b\Lambda_b}{\mu_b(\mu_b+\delta_b)}$ and determinant $D = 0$,

$$\lambda_\pm = \frac{\beta_b\Lambda_b}{2\mu_b(\mu_b+\delta_b)} \pm \sqrt{\left(\frac{\beta_b\Lambda_b}{2\mu_b(\mu_b+\delta_b)}\right)^2}$$

$$\lambda_+ = \frac{\beta_b\Lambda_b}{\mu_b(\mu_b+\delta_b)} \text{ or } \lambda_- = 0.$$

However, taking 0 as the basic reproduction number R_{AH} indicates that the disease is unable to spread into the system of the *avian-human BI model* at DFE state E^0_{AH}, which is not realistic. As a result, the basic reproduction number should be

$$R_{AH} = \frac{\beta_b\Lambda_b}{\mu_b(\mu_b+\delta_b)}, \tag{20}$$

which is the same as the basic reproduction number in (11). Thus, it is also locally asymptotically unstable with a different endemic equilibrium E^*_{AH}, (as shown in (18)), where

$$E^*_{AH} = (S^*_b, I^*_b, S^*_h, I^*_a) = (1.3950, 1166.4224, 280706.4850, 1342.6721). \tag{21}$$

4. Avian-human half-saturated incidence (HSI) model

As mentioned earlier in Section 1, several researchers have claimed that considering saturated incidence in modeling avian influenza is more suitable and realistic than assuming bilinear incidence (Gao et al., 2006; Yang et al., 2007).

That is why, in this section, we replaced the incidence rate from the bilinear to the half-saturated form. In the half-saturated incidence model, we added the half-saturation constants H_b and H_{bh} for the bird and human, respectively. The half-saturation constant is the density of infected individuals in the population as such that there is 50% chance for the individuals to contract avian influenza (Chong et al., 2014). We show below the half-saturated incidence model:

$$S_b'(t) = \Lambda_b - \mu_b S_b - \frac{\beta_b S_b I_b}{H_b + I_b} \tag{22}$$

$$I_b'(t) = \frac{\beta_b S_b I_b}{H_b + I_b} - (\mu_b+\delta_b) I_b \tag{23}$$

$$S_h'(t) = \Lambda_h - \mu_h S_h - \frac{\beta_{bh} S_h I_b}{H_{bh} + I_b} \tag{24}$$

$$I_a'(t) = \frac{\beta_{bh} S_h I_b}{H_{bh} + I_b} - (\mu_h + d) I_a. \tag{25}$$

To differentiate the HSI models presented in this section from the BI models presented in the previous section, we use lower case letters for the subscript of DFE, EE, and the basic reproduction number.

4.1. Stability analysis of the avian-only HSI model

Similarly to what we did in the avian-only BI model, we perform stability analysis to determine whether the basic reproduction number R_0 of the calculated DFE is locally asymptotically stable or not in the *avian-only HSI model*. For the *avian-only HSI model*, we take Equation (22) and Equation (23) into consideration.

4.1.1. Disease-free equilibrium, E_b^0

Letting $S_b'(t), I_b = 0$ in Equation (22):

$$S_b^0 = \frac{\Lambda_b}{\mu_b}.$$

Thus, the DFE of the *avian-only HSI model* is represented by

$$E_b^0 = \left(S_b^0, I_b^0\right) = \left(\frac{\Lambda_b}{\mu_b}, 0\right), \tag{26}$$

which is the same as the E_B^0 obtained in the avian-only BI model (shown in (5)).

4.1.2. Endemic equilibrium, E_b^*

Similarly to what we did in the EE of the avian-only BI model, $I_b \neq 0$ at EE and the EE of the *avian-only HSI model* is represented by

$$E_b^* = (S_b^*, I_b^*) = \left(\frac{H_b(\mu_b + \delta_b) + \Lambda_b}{\mu_b + \beta_b}, \frac{\beta_b \Lambda_b - H_b \mu_b (\mu_b + \delta_b)}{(\mu_b + \delta_b)(\mu_b + \beta_b)}\right). \tag{27}$$

4.1.3. Basic reproduction number, $R_{\bar{b}}$

Similarly to what we did in the avian-only BI model, we determine the transmission matrix **F** and transition matrix **V** to obtain the basic reproduction number $R_{\bar{b}}$ for DFE state of the *avian-only HSI model*. As a result, the basic reproduction number for DFE state of the *avian-only HSI model* is

$$R_{\bar{b}} = \mathbf{F}\mathbf{V}^{-1}\left(E_b^0\right) = \frac{\beta_b \Lambda_b}{\mu_b H_b (\mu_b + \delta_b)}. \tag{28}$$

Considering the parameter values collected in relevance to the H5N6 outbreak in the Philippines (as shown in Table 3), the basic reproduction number in (28) is then

$$R_{\bar{b}} = 0.0164, \tag{29}$$

indicating that the DFE in (26) is locally asymptotically stable. Since $R_{\bar{b}} < 1$, an endemic equilibrium of this model must be locally asymptotically unstable. We also have shown in Appendix A.2 that the global stability of the system at the given DFE is globally stable.

4.2. Stability analysis of the avian-human HSI model

We now consider the interaction between the population of the birds and humans. We use Equations (22)–(25) of the HSI model to obtain the basic reproduction number for the disease-free state of the *avian-human HSI model*.

4.2.1. Disease-free equilibrium, E_{ah}^0

Letting $S_h'(t), I_a = 0$ in Equation (24):

$$S_h^0 = \frac{\Lambda_h}{\mu_h}.$$

Thereby, the DFE of the *avian-human HSI model* is represented by

$$E_{ah}^0 = \left(S_b^0, I_b^0, S_h^0, I_a^0\right) = \left(\frac{\Lambda_b}{\mu_b}, 0, \frac{\Lambda_h}{\mu_h}, 0\right), \tag{30}$$

which is the same as the E_{AH}^0 obtained in the avian-human BI model (shown in (13)).

4.2.2. Endemic equilibrium, E_{ah}^*

Similarly to what we did in the EE of the avian-human BI model, $I_a \neq 0$ at EE and the EE of the *avian-human HSI model* is represented by the following:

$$\begin{aligned} E_{ah}^* &= (S_b^*, I_b^*, S_h^*, I_a^*) \\ &= \Bigg(\frac{H_b(\mu_b+\delta_b)+\Lambda_b}{\mu_b+\beta_b}, \frac{\beta_b\Lambda_b - H_b\mu_b(\mu_b+\delta_b)}{(\mu_b+\delta_b)(\mu_b+\beta_b)}, \\ &\quad \frac{\Lambda_h[H_{bh}(\mu_b+\delta_b)(\mu_b+\beta_b)+\beta_b\Lambda_b - H_b\mu_b(\mu_b+\delta_b)]}{D_1}, \\ &\quad \frac{\Lambda_h\beta_{bh}[\beta_b\Lambda_b - H_b\mu_b(\mu_b+\delta_b)]}{(\mu_h+d)D_1} \Bigg) \end{aligned} \tag{31}$$

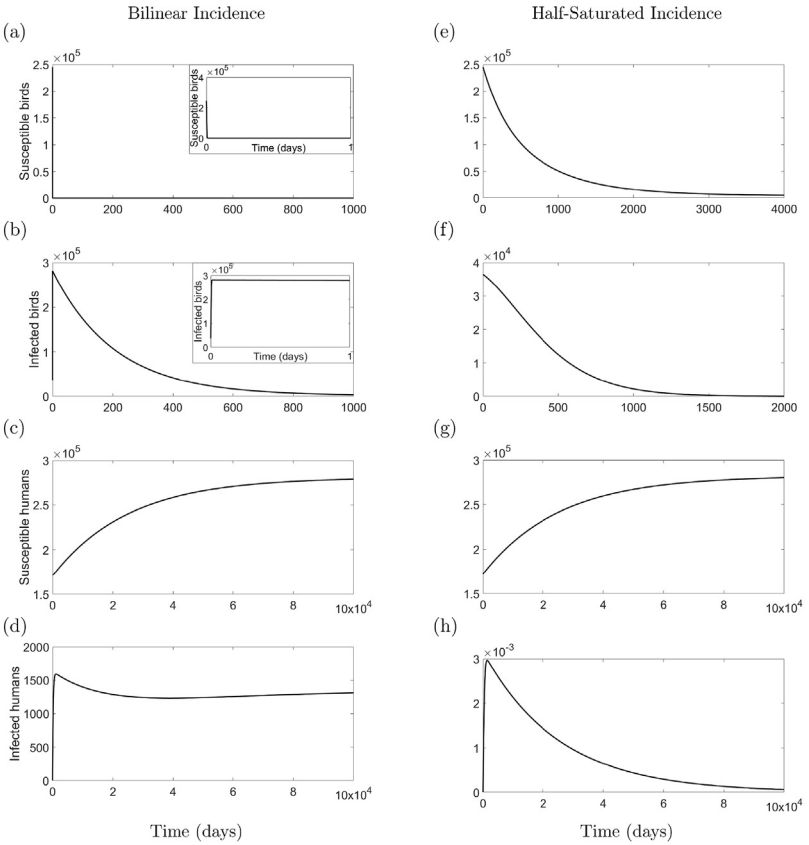

Fig. 2. State trajectories of the bilinear incidence and half-saturated incidence model. The figures in the left column represent the state trajectories of the BI (bilinear incidence) models, and the figures in the right correspond to that of HSI (half-saturated incidence) models. The parameter values and initial conditions that are used in both models are listed in Table 3.

where $D_1 = \mu_b(\delta_b + \mu_b)[H_{bh}\mu_h - H_b(\beta_{bh} + \mu_h)] + \beta_b[\beta_{bh}\Lambda_b + \mu_h(H_{bh}(\delta_b + \mu_b) + \Lambda_b)]$.

4.2.3. Basic reproduction number, R_{ah}

Similarly to what we did in the avian-human BI model, the basic reproduction number for DFE state of the *avian-human HSI model* is given by

$$R_{ah} = \frac{\beta_b \Lambda_b}{H_b \mu_b(\mu_b + \delta_b)}, \tag{32}$$

which is the same as the basic reproduction number in (28) (i.e. $R_{ah} = 0.0164$) and the DFE in (30) is

$$E^0_{ah} = \left(S^0_b, I^0_b, S^0_h, I^0_a\right) = (4120, 0, 282049.1591, 0). \tag{33}$$

At the given DFE, we have also shown that it is globally stable (see Appendix A.2).

5. The transmission dynamics of H5N6 in the Philippines

In this section, we compared the BI (presented in Section 3) and the HSI (presented in Section 4) models using the same set of parameters collected from the most recent H5N6 outbreak (OIE) in the Philippines. For both models, we set the initial values as $(S_b(0),\ I_b(0),\ S_h(0),\ I_a(0)) = (244956,\ 36485,\ 171977,\ 0)$ and the parameter values as those listed in Table 3. The simulations for both the BI and the HSI models are illustrated in Fig. 2.

For the BI model, we have shown that its endemic equilibrium point, $E^*_{AH} = (S^*_b,\ I^*_b,\ S^*_h,\ I^*_a) = (1.3950,\ 1166.4224,\ 280706.4850,\ 1342.6721)$ (as shown in (21)), is consistent to the steady state values derived from the simulations of S_b, I_b, S_h, and I_a (shown in the left column of Fig. 2). Similarly, for the HSI model, the disease-free equilibrium point, $E^0_{ah} = (S^0_b,\ I^0_b,\ S^0_h,\ I^0_a) = (4120,\ 0,\ 282049.1591,\ 0)$ (as shown in (33)), corresponds to the steady state values of the HSI model simulations (shown in the right column of Fig. 2).

It can be observed from the BI model simulations (left column of Fig. 2) that the moment when the birds were exposed to infection at time $t = 0$, the population of the susceptible birds (S_b illustrated by Fig. 2a) were converted to infected birds in less than a day (I_b as shown in zoomed plot in Fig. 2b). It is noteworthy to mention that this erratic change over night in the population of the infected birds caused by H5N6 is unrealistic.

As for its effect on the human population, the population of infected humans (shown in Fig. 2d) shoot up, slightly decreases and then reaches steady state at early time point. The human population infected by the disease has minimal effect on the susceptible human population (shown in Fig. 2c), since the population of infected humans (shown in Fig. 2d) is only 0.01% of the initial population of susceptible humans.

In the simulations of the HSI model (illustrated in the right column of Fig. 2), except for the I_b (Fig. 2f), the dynamics of the S_b (Fig. 2e), S_h (Fig. 2g), and I_a (Fig. 2h) are similar to that of the BI model (illustrated in the left column of Fig. 2).

The transmission dynamics of the HSI model, using the data collected in relation to the recent H5N6 outbreak in the Philippines (see Table 3), show that as the population of susceptible birds (Fig. 2e) decreased exponentially, the population of infected birds also (Fig. 2f) decreases. This is actually a reflection of the control strategy implemented by the Philippine government, which is culling of all poultry in the farm with reported H5N6 cases (OIE). This may be the reason why there was no reported case of infected human (as shown in Fig. 2g and h).

Comparing the transmission dynamics resulted from two types of incidence (see Fig. 2), namely the bilinear (BI) and half-saturated (HSI), the one generated using the HSI approach better mimics the actuality of the H5N6 outbreak in the Philippines on August 2017. Hence, from here on, the study and analysis will be focused on the effect of half-saturated incidence on the transmission dynamics of avian influenza.

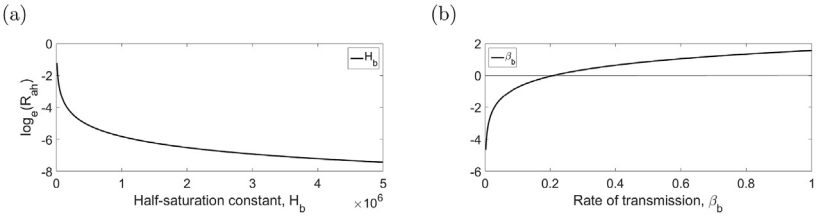

Fig. 3. Effect of half-saturation constant for birds with avian strain (a) and transmission coefficient (b) on the basic reproduction number.

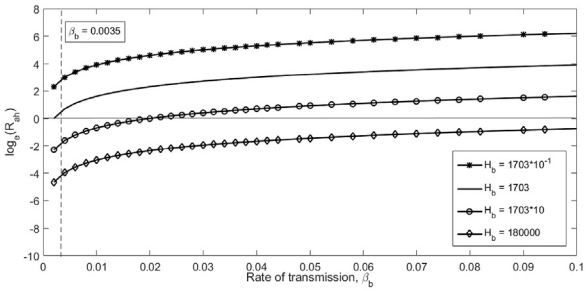

Fig. 4. The effect of the β_b on R_{ah}. We let $\beta_b \in [0, 0.1]$ so that we can indicate the original parameter value of β_b which is 0.0035.

6. Control strategies on endemic case

In this section, we investigated the effectiveness of the proposed control strategies when the outbreak becomes endemic. In order to do so, we will first modify the existing avian-human HSI model to be in accord to the endemic condition (shown in Section 6.1), followed by the implementation of non-medicinal (personal protection in 6.2 and poultry isolation in Section 6.3) medicinal (poultry vaccination in Section 6.4) control strategies.

6.1. Endemic case of avian-only HSI model

To establish a model with endemic scenario, we first recall a concept on basic reproduction number, that is, "*the disease will die off when* $\log_e(R_{ah}) \leq 0$ *and otherwise persist if* $\log_e(R_{ah}) > 0$". We used a semi-log plot for R_{ah} with respect to H_b and β_b to bring out features in the simulations that would not easily be seen if both variables had been plotted linearly (Bourne). In this section, we first examine the effect of H_b (Fig. 3a) and β_b (Fig. 3b) on R_{ah} (shown in (32)) of the avian-human HSI model.

As shown in Fig. 3a, $\log_e(R_{ah}) < 0$ for any values of H_b. Whereas, in Fig. 3b, $\log_e(R_{ah})$ switches from < 0 to > 0 when $\beta_b \geq 0.2$. This implies that changing half-saturation constant has no effect in switching the HSI model from disease-free to endemic (which is the goal of this section), but the rate of transmission has.

To further examine at what point of negligence in protective measures in reducing the chance of disease contraction in birds (i.e. H_b) will result to endemic condition, we first calculated the H_b assuming that R_{ah} shown in (31) is > 1 (making the model endemic) while fixing the other parameter values as listed in Table 3:

$$\begin{aligned} R_{ah} &= \frac{\beta_b \Lambda_b}{H_b \mu_b (\mu_b + \delta_b)} > 1 \\ \frac{2953.3764}{H_b} &> 1 \\ H_b &< 2953.3764 \\ H_b^* &= 2953.3764 \approx 2953. \end{aligned}$$

we found that the upper bound of $H_b = 2953$ for the set of parameters listed in Table 3.

When we investigated the influence of transmission coefficient β_b on R_{ah} with increasing values of H_b (as shown in Fig. 4), we observed that for $H_b \leq 1703$ (two upper curves in Fig. 4), $\log_e(R_{ah})$ is always > 0, in which the model will never reach the

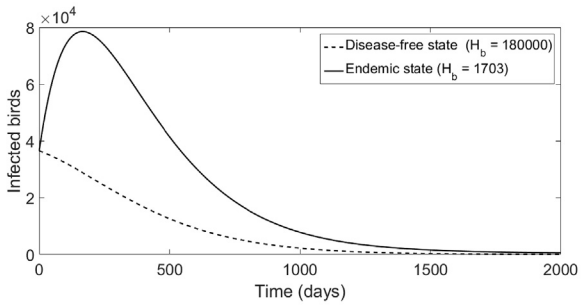

Fig. 5. Comparison between the effects of avian influenza transmission dynamics in disease-free state and endemic state of half-saturated incidence model on infected birds.

state of disease free. On the other hand, for $H_b > 1703$ (bottom two curves of Fig. 4), depending on the value of β_b, the model can switch from disease-free to endemic state.

As a result of the rigorous investigations, by changing the half saturation constant for birds with avian strain H_b from 180,000 (broken-line in Fig. 5) to 1,703 (solid-line in Fig. 5) on the existing avian-human HSI model, we had successfully shifted the disease-free state of the model into an endemic state, as such that

$$E^*_{ah} = (S^*_b, I^*_b, S^*_h, I^*_a) = (2869.6824, 354.1001, 282049.1557, 0.0034)$$

and

$$R_{ah} = 1.7342. \tag{34}$$

The endemic condition of avian influenza is reflected by the huge increase in the population of infected birds shown in Fig. 5

6.2. Personal protection

Lack of personal protections such as consumption of uncooked infected poultry goods, exposure to infected dust, and poor hygiene are some possible causes of contracting avian influenza (Katz et al.,). The health-care workers (HCWs) are the ones that have a higher risk for contracting the disease since they have numerous contact with infected birds (Avian influenza). Converting the new scale for the β_{bh} to $(1 - cq)\beta_{bh}$, we examine the effect of personal protection on controlling the disease transmission in humans. Taking into account of the total population of the birds (i.e. $N_b = S_b + I_b$), the model below has been modified (using the new scale) with the concept of personal protection:

$$S_h{}'(t) = \Lambda_h - \mu_h S_h - (1 - cq)\frac{\beta_{bh} S_h I_b}{H_{bh} + I_b} \tag{35}$$

$$I_a{}'(t) = (1 - cq)\frac{\beta_{bh} S_h I_b}{H_{bh} + I_b} - (\mu_h + d) I_a \tag{36}$$

where $c, q \in [0, 1]$, c is the percentage of population that followed personal protection and q is the effectiveness of personal protection.

6.2.1. Stability analysis of the avian-human personal protection model

While taking Equations (22) and (23) of Section 4 into consideration, we use Equations (35) and (36).

The DFE of the *avian-human personal protection model* is

$$E^0_{PP} = \left(S^0_b, I^0_b, S^0_h, I^0_a\right) = \left(\frac{\Lambda_b}{\mu_b}, 0, \frac{\Lambda_h}{\mu_h}, 0\right), \tag{37}$$

which is the same as E^0_{ah} (shown in (30) of Section 4.2).

Since the representation of $S_b{}'(t)$ and $I_b{}'(t)$ under personal protection is the same as those in HSI model, S^*_b and I^*_b of E^*_{PP} is the same as shown in (31) of Section 4.2. The EE of the *avian-human personal protection model* is

$$\begin{aligned} E^*_{PP} &= (S^*_b, I^*_b, S^*_h, I^*_a) \\ &= \left(\frac{H_b(\mu_b + \delta_b) + \Lambda_b}{\mu_b + \beta_b}, \frac{\beta_b \Lambda_b - H_b \mu_b(\mu_b + \delta_b)}{(\mu_b + \delta_b)(\mu_b + \beta_b)}, \right. \\ &\quad \frac{\Lambda_h[\beta_b \Lambda_b - H_b \mu_b(\delta_b + \mu_b) + H_{bh}(\beta_b + \mu_b)(\delta_b + \mu_b)]}{D_2}, \\ &\quad \left. - \frac{\beta_{bh}(cq - 1)\Lambda_h[\beta_b \Lambda_b - H_b \mu_b(\delta_b + \mu_b)]}{(d + \mu_h) D_2}\right) \end{aligned} \tag{38}$$

where $D_2 = \mu_b(\delta_b + \mu_b)[\beta_{bh}(cq - 1)H_b - H_b\mu_h + H_{bh}\mu_h] + \beta_b[\beta_{bh}(\Lambda_b - cq\Lambda_b) + \mu_h[H_{bh}(\delta_b + \mu_b) + \Lambda_b]]$ and E^*_{PP} is similar to E^*_{ah} (shown in (31)) of Section 4.2.

The transmission matrix **F** of the *avian-human personal protection model* is

$$\mathbf{F} = \begin{bmatrix} \dfrac{\beta_b S_b H_b}{(H_b + I_b)^2} & 0 \\ \dfrac{(1-cq)\beta_{bh} S_h H_{bh}}{(H_{bh} + I_b)^2} & 0 \end{bmatrix}. \tag{39}$$

Substituting DFE in (37) into matrix **F** in (39), this leads to

$$\begin{aligned} \mathbf{F}\mathbf{V}^{-1}\left(E^0_{PP}\right) &= \begin{bmatrix} \dfrac{\beta_b \Lambda_b}{H_b \mu_b} & 0 \\ \dfrac{(1-cq)\beta_{bh}\Lambda_h}{H_{bh}\mu_h} & 0 \end{bmatrix} \begin{bmatrix} \dfrac{1}{\mu_b + \delta_b} & 0 \\ 0 & \dfrac{1}{\mu_h + d} \end{bmatrix} \\ &= \begin{bmatrix} \dfrac{\beta_b \Lambda_b}{H_b \mu_b (\mu_b + \delta_b)} & 0 \\ \dfrac{(1-cq)\beta_{bh}\Lambda_h}{H_{bh}\mu_h(\mu_b + \delta_b)} & 0 \end{bmatrix}. \end{aligned}$$

Even though $\frac{(1-cq)\beta_{bh}\Lambda_h}{H_{bh}\mu_h(\mu_b+\delta_b)}$ is not the basic reproduction number R_{PP}, we let $R_{PP} = \frac{(1-cq)\beta_{bh}\Lambda_h}{H_{bh}\mu_h(\mu_b+\delta_b)}$ to examine the effect of H_{bh} and β_{bh} on the disease in the population of humans for the moment. Substituting the original parameter values in Table 3 into R_{PP},

$$\begin{aligned} R_{PP} &= \frac{(1-cq)\beta_{bh}\Lambda_h}{H_{bh}\mu_h(\mu_b + \delta_b)} \\ &= (1-cq)7.88925 \times 10^{-8} \end{aligned}$$

in which the value of R_{PP} is extremely small for the disease to occur. Thus, we first determine the threshold value of H_{bh} to see if it is possible to occur in an endemic scenario. Solving for H_{bh} in R_{PP}, the threshold value H^*_{bh} is given by

$$\begin{aligned} R_{PP} &> 1 \\ \frac{(1-cq)\beta_{bh}\Lambda_h}{H_{bh}\mu_h(\mu_b + \delta_b)} &> 1 \\ \frac{0.0094671(1-cq)}{H_{bh}} &> 1 \\ H_{bh} &< 0.0094671(1-cq) \end{aligned}$$

which is impossible since R_{PP} will be undefined if $H^*_{bh} = 0$. For this reason, we find the minimum value of β^*_{bh} while setting the values of other variables fixed:

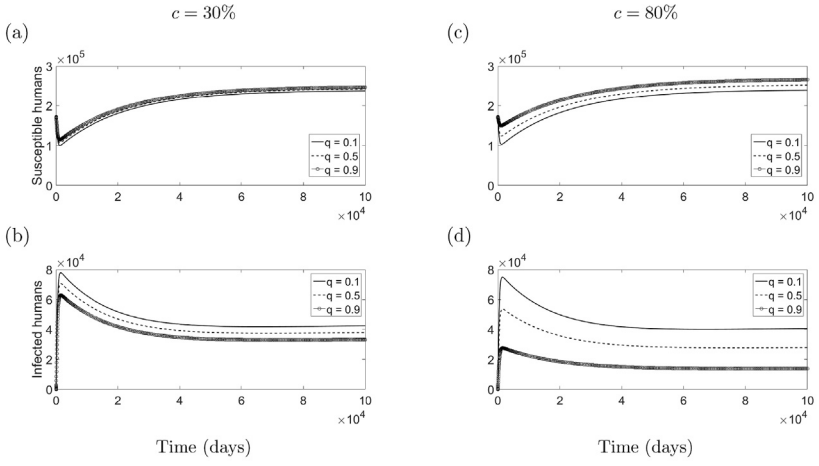

Fig. 6. State trajectories of human personal protection model.

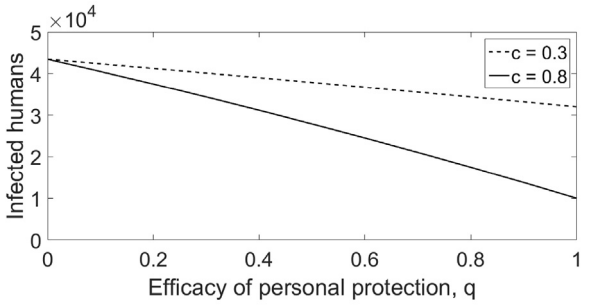

Fig. 7. The effects of personal protection on infected humans with avian strain.

$$\begin{aligned} &\frac{(1-cq)\beta_{bh}\Lambda_h}{H_{bh}\mu_h(\mu_b+\delta_b)} > 1 \\ &485.928(1-cq)\beta_{bh} > 1 \\ &\beta_{bh} > \frac{0.00205792}{(1-cq)}. \end{aligned} \tag{40}$$

For simplicity, we let $\beta^*_{bh} = 2.5 \times 10^{-3}$. Substituting the new value of β^*_{bh} into (40),

$$R_{PP} = 1.21482(1-cq)$$

and the EE of *avian-human personal protection model* (shown in (38)) is

$$E^*_{PP} = (S^*_b, I^*_b, S^*_h, I^*_a) = \left(2869.6824, 354.1001, \frac{1.5182 \times 10^6}{6.3826 - cq}, \frac{282048.7254 - 282048.7254cq}{6.3826 - cq}\right).$$

6.2.2. Impact of personal protection on humans

While the population of susceptible humans (S_h) decreased due to infection, the implementation of personal protection prevented S_h from continually declining; thus, leading to an increase in S_h until it reaches its steady state (as shown in Fig. 6a and c). When there were more people that employed personal protection (as shown in Fig. 6c), the total number of susceptible humans at the final state was higher than what was shown in Fig. 6a.

No matter the efficacy of the personal protection (q), if the overall population (c) is not practicing personal protection, it does not have any drastic effect on reducing the infected humans (as shown in Fig. 6b). On the other hand, when 80% of the population engaged in personal protection, the population of infected humans decreases as q increases (as shown in Fig. 6d).

Consistent to what is shown in Fig. 6b and d, Fig. 7 presents that if $c = 0.3$ (i.e. only 30% of the population followed personal protection) and as q (efficacy of personal protection) increases, there is only a minimal decrease in the number of infected humans.

Aside from implementing personal protection and ensuring its efficacy, it is also important that the strategy is employed by a huge percentage of the population to be able to effectively decrease the number of infected humans.

6.3. Isolation strategy

Even if the isolation strategy may not eliminate the disease completely, it can minimize the rate of disease contraction and spread (Gumel, 2009; WHO). Hence, in this section, given an endemic scenario in the model, we included the population of the isolated birds (denoted by $T_b(t)$) and that of recovered birds (denoted by $R_b(t)$), given that the isolation method is effective (as shown in Fig. 8). Since the isolation of the birds has no effect in disease transmission on the population of the humans, we only take the HSI avian-only model into consideration. However, in order to investigate how the isolation strategy works in minimizing the disease contraction and spread, the representation of $I_b'(t)$ for the infected birds is modified. We added γ_b representing the recovery rate of infected birds and ψ_b describing the rate of isolation of birds with avian flu (i.e. the number of identified infected birds from the total bird population that has been put into isolation). For convenience, we let $\gamma_b = 0.003$ and below is the representation model for bird isolation:

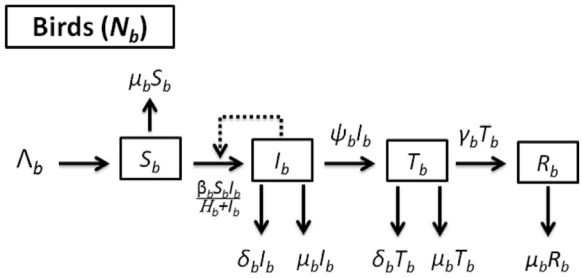

Fig. 8. The isolation model of H5N6 virus transmission in birds.

$$S_b'(t) = \Lambda_b - \mu_b S_b - \frac{\beta_b S_b I_b}{H_b + I_b} \tag{41}$$

$$I_b'(t) = \frac{\beta_b S_b I_b}{H_b + I_b} - (\mu_b + \delta_b + \psi_b) I_b \tag{42}$$

$$T_b'(t) = \psi_b I_b - (\mu_b + \delta_b + \gamma_b) T_b \tag{43}$$

$$R_b'(t) = \gamma_b T_b - \mu_b R_b. \tag{44}$$

6.3.1. Stability analysis of the avian-only isolation model

We use Equations (41)–(44) of isolation model to perform stability analysis where the new total bird population $N_b = S_b + I_b + T_b + R_b$.

Letting $T_b'(t) = 0$ and $I_b = 0$ in Equation (43),

$$\begin{aligned} T_b'(t) &= \psi_b I_b - (\mu_b + \delta_b + \gamma_b) T_b \\ T_b^0 &= 0. \end{aligned}$$

Thereby, the DFE of the *avian-only isolation model* is represented by

$$E_T^0 = \left(S_b^0, I_b^0, T_b^0, R_b^0\right) = \left(\frac{\Lambda_b}{\mu_b}, 0, 0, 0\right). \tag{45}$$

and the EE of the *avian-only isolation model* is

$$\begin{aligned} E_T^* &= (S_b^*, I_b^*, T_b^*, R_b^*) \\ &= \left(\frac{H_b(\delta_b + \mu_b + \psi_b) + \Lambda_b}{\beta_b + \mu_b}, \frac{\beta_b \Lambda_b - H_b \mu_b (\delta_b + \mu_b + \psi_b)}{(\beta_b + \mu_b)(\delta_b + \mu_b + \psi_b)}, \right. \\ &\frac{\beta_b \Lambda_b \psi_b - H_b \mu_b \psi_b (\delta_b + \mu_b + \psi_b)}{(\beta_b + \mu_b)(\gamma_b + \delta_b + \mu_b)(\delta_b + \mu_b + \psi_b)}, \\ &\left. \frac{\gamma_b \psi_b [\beta_b \Lambda_b - H_b \mu_b (\delta_b + \mu_b + \psi_b)]}{\mu_b (\beta_b + \mu_b)(\gamma_b + \delta_b + \mu_b)(\delta_b + \mu_b + \psi_b)}\right) \end{aligned} \tag{46}$$

such that

$$\begin{aligned} E_T^* &= (S_b^*, I_b^*, T_b^*, R_b^*) \\ &= \left(352064.9451\psi_b + 2869.6824, \frac{1.7128 - 482.2807\psi_b}{\psi_b + 0.0048}, \right. \\ &\left. \frac{\psi_b (218.5498 - 61539.3576\psi_b)}{\psi_b + 0.0048}, \frac{\psi_b (478.6242 - 134771.1932\psi_b)}{\psi_b + 0.0048}\right) \end{aligned}$$

where $\psi_b \in [0, 1]$.

The transmission matrix **F** of the *avian-only isolation model* be defined by

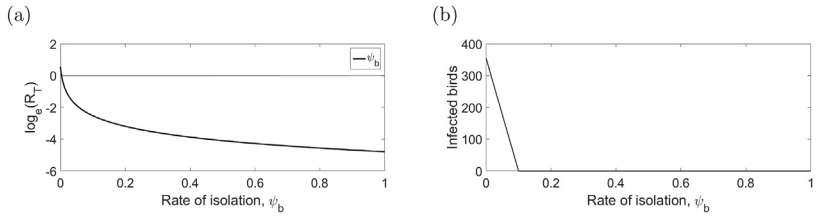

Fig. 9. Significance of ψ_b on controlling the disease. As shown in (a), the disease will persist if the rate of isolation is less than 3.6×10^{-3}.

$$\mathbf{F} = \left[\frac{\partial\left(\frac{\beta_b S_b I_b}{H_b + I_b}\right)}{\partial I_b}\right] = \left[\frac{\beta_b S_b H_b}{(H_b + I_b)^2}\right]. \tag{47}$$

Substituting DFE in (45) into matrix **F** in (47), we arrived at

$$R_T = \mathbf{F}\mathbf{V}^{-1} = \frac{\beta_b \Lambda_b}{\mu_b H_b(\mu_b + \delta_b + \psi_b)} = \frac{0.0084}{\psi_b + 0.0048}. \tag{48}$$

6.3.2. Impact of isolation on population of the birds

To start, we first solve for ψ_b in the basic reproduction number in (48), such that the threshold value ψ_b^* is

$$R_T = \frac{0.0084}{\psi_b + 0.0048} > 1$$
$$\psi_b < 3.6 \times 10^{-3}$$
$$\psi_b^* = 3.6 \times 10^{-3}.$$

This implies that the disease will persist if the rate of isolation is less than 3.6×10^{-3} (as illustrated in Fig. 9a). Also, at this given interval, it will be crucial to control and prevent the disease. As this trend of increasing isolation rate continues, it will eventually lead to disease elimination (as shown in Fig. 9a).

However, as shown in Fig. 9b, as the values of ψ_b become > 0.1, the corresponding populations of the infected birds at the equilibrium state are indifferent. It may suggest that the isolation rate is effective in controlling the infection when ψ_b lies between 0 and 10% but has no effect on minimizing the population of infected birds when greater than 10%.

We now consider the case when $\psi_b \in \{0.001, 0.005, 0.009\}$. Increasing the isolation rate (ψ_b) from 0.001 to 0.009 does not have significant effect on the population of susceptible birds (as shown in Fig. 10a). What is noticeable (in Fig. 10b) is that there is a drastic decrease in the population of infected birds as we increased ψ_b from 0.001 to 0.009. Increasing ψ_b will increase the number of infected birds that were put into isolation instantly but minimizes more number of isolated birds eventually (as shown in Fig. 10c). The dynamics of the recovery of birds (Fig. 10d) is the same as that of isolated birds. However, because it takes some time for the isolated birds to recover, we observe delay on the time when the number of recovered birds reaches its peak (see Fig. 10d) as compared to the time the population of isolated birds reaches its peak (see Fig. 10c). Moreover, it can be viewed that when $\psi_b = 0.009$, about 85% of the isolated birds recovered from avian influenza (Fig. 11).

6.4. Vaccination strategy

To prevent the spread of disease in animals, researchers had developed the adjuvanted heterologous H5N6 avian influenza virus vaccine (Joob & Viroj, 2015). It is only applied to animals and has not been tested on humans. For humans, there are vaccines that may be used to control and prevent subtype H5 infection but there is no particular vaccine against H5N6 (Korea Freezes Poultry Shipments). For this reason, we will implement the vaccination, as control strategy, into the birds instead of the human population. We add an equation representing the dynamics of vaccinated birds and denote it by $V_b(t)$. Furthermore, we modified the representation of $S_b'(t)$ and $I_b'(t)$ (shown in Equations (22) and (23) of Section (4)) by integrating the effect of vaccine coverage (denoted by p) and efficacy of the vaccine (denoted by ϕ), respectively:

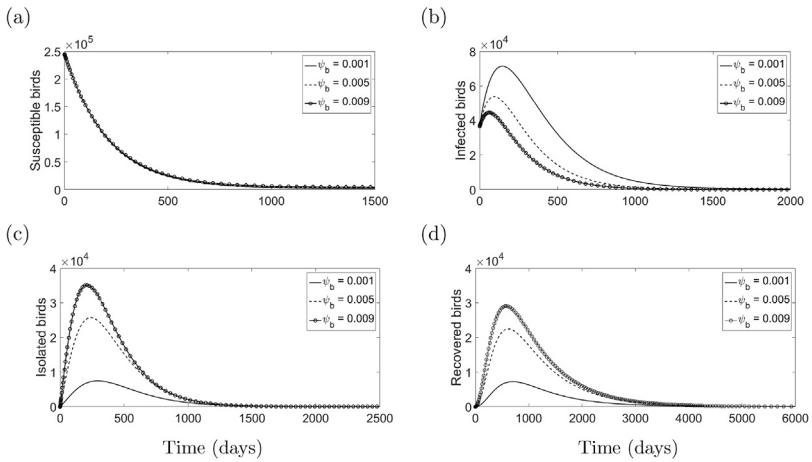

Fig. 10. State trajectories of avian-only isolation model.

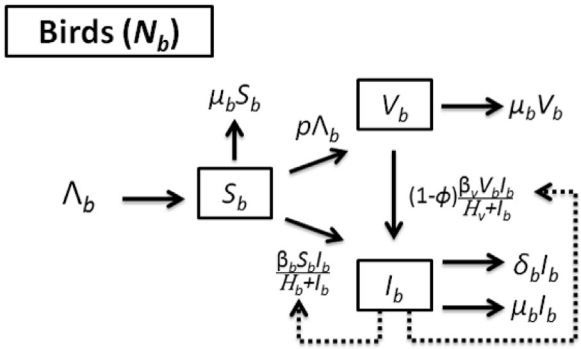

Fig. 11. The vaccination model of H5N6 virus transmission in birds.

$$S_b'(t) = (1-p)\Lambda_b - \mu_b S_b - \frac{\beta_b S_b I_b}{H_b + I_b} \tag{49}$$

$$V_b'(t) = p\Lambda_b - (1-\varphi)\frac{\beta_v V_b I_b}{H_v + I_b} - \mu_b V_b \tag{50}$$

$$I_b'(t) = \frac{\beta_b S_b I_b}{H_b + I_b} + (1-\varphi)\frac{\beta_v V_b I_b}{H_v + I_b} - (\mu_b + \delta_b) I_b. \tag{51}$$

where β_v represents the rate at which vaccinated birds contract avian influenza and H_v indicates the half-saturation constant for vaccinated birds. For convenience, we assume that the vaccination lessens the chance of contracting the avian influenza by 50% than that of the susceptible birds that did not receive vaccination. Hence, we let $\beta_v = 1.734 \times 10^{-3}$ and $H_v = 850$.

6.4.1. Stability analysis of the avian-only vaccination model

We perform stability analysis on the vaccination model where the total bird population $N_b = S_b + I_b + V_b$. Letting $S_b'(t)$, $I_b = 0$ in Equation (49),

$$S_b'(t) = (1-p)\Lambda_b - \mu_b S_b - \frac{\beta_b S_b I_b}{H_b + I_b}$$

$$S_b^0 = \frac{(1-p)\Lambda_b}{\mu_b}.$$

Letting $V_b'(t)$, $I_b = 0$ in Equation (50),

$$V_b'(t) = p\Lambda_b - (1-\varphi)\frac{\beta_v V_b I_b}{H_v + I_b} - \mu_b V_b$$

$$V_b^0 = \frac{p\Lambda_b}{\mu_b}.$$

Thus, the DFE of the *avian-only vaccination model* is represented by

$$E_{V_b}^0 = \left(S_b^0, V_b^0, I_b^0\right) = \left(\frac{(1-p)\Lambda_b}{\mu_b}, \frac{p\Lambda_b}{\mu_b}, 0\right); \tag{52}$$

and the corresponding EE is provided in the Supplementary Materials.

Since the population of vaccinated birds (V_b) belongs to the susceptible class (S_b), the rate of new infection is $\frac{\beta_b S_b I_b}{H_b+I_b} + (1-\varphi)\frac{\beta_v V_b I_b}{H_v+I_b}$. Therefore, the transmission matrix $\mathbf{F}$ of the *avian-only vaccination model* is defined by

$$\begin{aligned}\mathbf{F} &= \left[\frac{\partial\left(\frac{\beta_b S_b I_b}{H_b+I_b} + (1-\varphi)\frac{\beta_v V_b I_b}{H_v+I_b}\right)}{\partial I_b}\right] \\ &= \left[\frac{\beta_b S_b H_b}{(H_b+I_b)^2} + (1-\varphi)\frac{\beta_v V_b H_v}{(H_v+I_b)^2}\right].\end{aligned} \tag{53}$$

Substituting DFE in (52) into $\mathbf{F}$ in (53),

$$\begin{aligned}\mathbf{F}\left(E_{V_b}^0\right) &= \left[\frac{\beta_b S_b}{H_b} + (1-\varphi)\frac{\beta_v V_b}{H_v}\right] \\ &= \frac{\Lambda_b}{\mu_b}\left[\frac{\beta_b(1-p)}{H_b} + (1-\varphi)\frac{p\beta_v}{H_v}\right]\end{aligned}$$

and

$$\mathbf{V}^{-1} = \frac{1}{(\mu_b+\delta_b)}.$$

Consequently,

$$R_{V_b} = \mathbf{F}\mathbf{V}^{-1} = \frac{\Lambda_b}{\mu_b(\mu_b+\delta_b)}\left[\frac{\beta_b(1-p)}{H_b} + (1-\varphi)\frac{p\beta_v}{H_v}\right] \tag{54}$$

and

$$R_{V_b} = p(0.0031 - 1.7373\varphi) + 1.7342. \tag{55}$$

As we can observe in Fig. 12, R_{V_b} decreases if both the percentage of the vaccinated population (p) and the efficacy of the vaccine (φ) increases. Furthermore, the disease will persist when $p, \varphi \leq 0.4$.

6.4.2. Impact of vaccination on birds

After running the vaccination strategy model, we have shown in Fig. 13 that if we increase the vaccination coverage (p) and efficacy of the vaccine (φ), there is no significant change in the population of susceptible birds (S_b) (Fig. 13a and d) and infected population of the birds (Fig. 13c and f). It is interesting to observe that the vaccination (Fig. 13b and e) appears to have

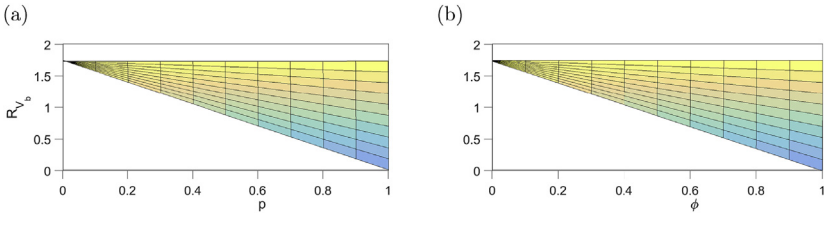

Fig. 12. Plots of the basic reproduction number R_{V_b} highlighting R_{V_b} versus p (a) and ϕ (b), respectively.

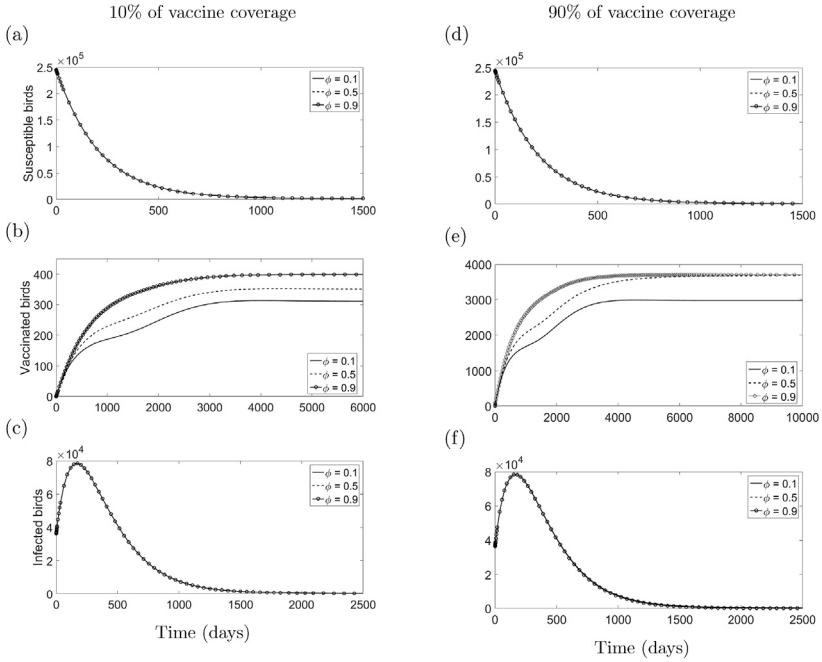

Fig. 13. State trajectories of avian-only vaccination model.

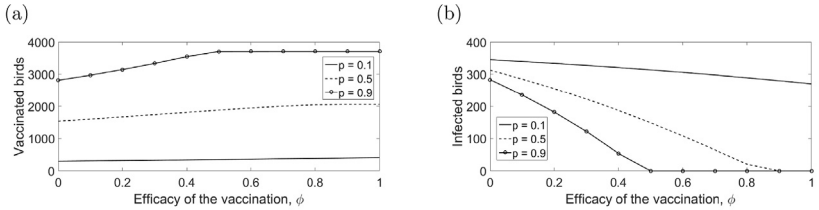

Fig. 14. Significance of p and ϕ on the total number of vaccinated (a) and infected birds (b).

no significant effect in reducing the population of infected birds no matter how efficient the vaccine is. For this reason, we investigated the role of p and ϕ on the population of vaccinated and infected birds in depth (as shown in Figure 14).

We first examined in Fig. 14 the importance of the efficacy of the vaccination (ϕ) on the equilibrium state of the vaccinated and infected birds with different values of p (i.e. the percentage of the vaccinated birds). With only 10% of the bird population being vaccinated (i.e. $p = 0.1$), even with higher efficacy of the vaccination, it does not remarkably reduce the population of the infected birds. However, with wider coverage of vaccinated birds (where $p = 0.9$) and an incremented ϕ, the number of vaccinated birds at equilibrium state increases and then stabilizes (see Fig. 14a); while the population of the infected birds at the equilibrium state reduces drastically only for $\varphi < 0.5$ (see Fig. 14b). Nevertheless, the populations of the infected birds at the equilibrium state are indifferent when the efficacy of the vaccination is higher than 50% despite that 90% of the particular population received vaccine (as shown in Fig. 14a and b).

Overall, we have shown that the prevalence rate plays more significant role as compared to the efficacy of the vaccine. No matter how effective the vaccine is, if the majority of the population is not vaccinated, it is hard to control and prevent the infection.

Table 2
Summary of basic reproduction numbers in infected birds, where l.a.s and l.a.u stands for locally asymptotically stable and unstable, respectively.

Scenarios	R_0 shown in	Value	Result
Avian-Only BI	(11)	2953.3764	l.a.u
Avian-Only HSI	(28)	0.0164	l.a.s
Avian-Only HSI (Endemic Case Section 6.1)	(34)	1.7342	l.a.u (when $H_b = 1703$)
Avian-Only Isolation	(48)	$\frac{0.0084}{\psi_b + 0.0048}$	l.a.u (when $\psi_b < 3.6 \times 10^{-3}$)
Avian-Only Vaccination	(54)	$p(0.0031 - 1.7373\varphi) + 1.7342$	l.a.u (when $p, \varphi \leq 0.4$)

7. Summary and conclusion

To examine the transmission dynamics of avian influenza from birds to humans, we formed a bilinear incidence avian-human model and a half-saturated incidence avian-human model. After comparing the state trajectories of the two models as aforementioned above, the simulations of half-saturated incidence model resembled the reality of H5N6 outbreak that occurred in the Philippines in August 2017. We first implemented personal protection on humans into our model to investigate its effect on reducing the infected humans during the outbreak of the avian influenza. And as a better alternative to culling the domestic birds to control and reduce the spread of avian influenza, we modeled the efficacy of implementing isolation and vaccination to the birds.

From the outcomes that we have achieved (shown in Table 2), the disease will persist when $p, \varphi \leq 0.4$ in vaccination strategy while the current state is already endemic when $\psi_b < 3.6 \times 10^{-3}$ in isolation strategy. Even if the prevalence rate of the vaccination (p) plays more important role in controlling the transmission of avian influenza than the efficacy of the vaccine (φ) (shown in Fig. 14), there is a need to invest more money, time, and effort in order to reduce the avian infection in domestic poultry. For the non-medicinal strategies (isolation strategy and personal protection), we were able to detect a significant decrease in the total number of infected individuals. Despite the fact that the rate of isolation is tremendously small for the avian influenza to occur (shown in Table 2), the (ψ_b) rate of isolation merely demands no more than 10% (shown in Fig. 9b) while it requires more attempt to increase the (p) prevalence rate of the vaccination and (φ) efficacy of the vaccine (shown in Fig. 14b) to minimize the total number of infected birds. Therefore, the isolation strategy is more preferable choice which is cost effective than the vaccination strategy.

If there is an outbreak of avian influenza, we recommend isolation strategy as a solution to control the transmission of avian influenza since the slaughter of domestic birds brings financial damage not only to the farmers but also to the industry of poultry as well (Avian flu poultry ban partially lifted). The Food and Agriculture Organization of the United Nations (FAO) suggests that after isolating the infected birds from the remaining domestic poultry that are kept, one should inform the local veterinary officials that are nearby at once. Furthermore, wearing protective gloves is crucial before handling infected poultry (Avian Flu). However, if ever the humans contract the avian flu transmitted through the birds, we propose personal protection to prevent the disease transmission among humans as well. In Singapore, the personal protection was confirmed to be successful when it was properly executed (Hospital Influenza Working Group, 2009). As a final point, the isolation strategy would offer greater benefits in controlling the transmission of avian influenza.

Acknowledgement

AL held a research fellowship from De La Salle University and would like to acknowledge the support of the Universitys Research Coordination Office.

Appendices

A. Preliminary concepts

A.1. R_0 calculations

R_0 is the basic reproduction number that verifies whether the disease can invade the population or not. The threshold of R_0 is 1 such that the disease will remain if $R_0 > 1$ while the disease will cease to exist if $R_0 \leq 1$. To compute R_0, we use the approach of (Diekmann et al., 1990; Jones, 2017; Van den Driessche & Watmough, 2002).

First, we have the vector $\bar{x} = [x_1, \ldots, x_n]^T$, where $i = 1, \ldots, n$ (number of compartments) and each x_i represents the number of individuals in each corresponding ith class. For example, given that we have four compartments based on Equations (1)–(4) in Section 3, $\bar{x} = [S_b(t), I_b(t), S_h(t), I_a(t)]^T$. However, since we are only interested in the infectious classes, we let $\bar{x} = [I_b(t), I_a(t)]^T$ in our paper instead. $F_i(\bar{x})$ gives us the new rate infections in the ith class coming from its corresponding susceptible compartment (in this case, either S_b or S_h). Finally, $V_i(\bar{x}) = V_i^-(\bar{x}) - V_i^+(\bar{x})$, where $V_i^+(\bar{x})$ describes the individuals that shifted into the ith infectious class from any other compartments except the susceptible class while $V_i^-(\bar{x})$ represents the individuals that are removed from the ith infectious class. Once we obtained $F_i(\bar{x})$ and $V_i(\bar{x})$, we can solve for the transmission matrix $\mathbf{F}$ and transition matrix $\mathbf{V}$ as shown below,

$$\mathbf{F} = \left[\frac{\partial F_i(x_0)}{\partial x_j}\right], \mathbf{V} = \left[\frac{\partial V_i(x_0)}{\partial x_j}\right]$$

where x_0 indicates the state at disease-free equilibrium and $\mathbf{F}$ and $\mathbf{V}$ are the Jacobian matrices of $F_i(\bar{x})$ and $V_i(\bar{x})$ at DFE state, respectively.

After computing matrix **F** and **V**, we determine the dominant eigenvalue of $\mathbf{FV}^{-1}$ to get R_0. The formula for finding the eigenvalues of $\mathbf{FV}^{-1}$ is given below,

$$\lambda_{\pm} = \frac{T}{2} \pm \sqrt{\left(\frac{T}{2}\right)^2 - D}$$

where T is the trace and D is the determinant of $\mathbf{FV}^{-1}$.

A.2. Global stability of the disease-free equilibrium (DFE)

In the following, we show that the DFE (E_*^0) is *globally stable* for avian-only and avian-human model of half-saturated incidence (HSI), and avian-only model of isolation strategy. Before we investigate whether or not the DFE $\left(E_b^0\right)$ of HSI model is *globally stable*, we first define a *Lyapunov function*.

Lyapunov function (Bressan; Weisstein)

Given that x_0 represents the state at DFE for differential equation $x' = f(x)$, a continuous and differentiable function $L = L(x)$ defined for x in a neighborhood of x_0 is *Lyapunov* if the following conditions are satisfied:

- positive definite (i.e. $L(x_0) = 0$ and $L(x) > 0$, $\forall x \neq x_0$)
- $\frac{\partial L(x)}{\partial x} f(x) \leq 0$ at every point $x \in \mathbb{R}^n$, where $x' = f(x)$

such that $\frac{d}{dt}L(x(t)) = \frac{\partial L(x(t))}{\partial x(t)} f(x(t)) \leq 0$ or $L(x(t))$ is non-increasing in time. It is said that x_0 is stable if a Lyapunov function exists and asymptotically stable if $L(x(t))$ is strictly decreasing.

LaSalle's invariance principle (Bressan)

x_0 is asymptotically stable if the existence of Lyapunov function L is satisfied and for any initial point $y \neq x_0$, the function $t \mapsto L(\varphi(t, y))$ is nonconstant.

Theorem A.1. (Global stability of the DFE for the avian-only HSI model (Chong et al., 2014)). *Letting* $E_b^0 = (S_b^0, I_b^0)$, *the DFE* (E_b^0) *is said to be globally stable in the interior* $\Gamma_b = \{(S_b, I_b) \in \mathbb{R}_+^2 : S_b, I_b \leq N_b\}$ *if* $R_{\bar{b}} < 1$.

Proof. We consider a Lyapunov function, $L(S_b, I_b) = \frac{\Lambda_b}{\mu_b H_b(\mu_b + \delta_b)} I_b$. At the DFE of HSI model, we have $L(S_b^0, I_b^0) = L\left(\frac{\Lambda_b}{\mu_b}, 0\right) = 0$, and its derivative is

$$\begin{aligned}
\frac{dL}{dt} &= \frac{\Lambda_b}{\mu_b H_b(\mu_b + \delta_b)} I_b' \\
&= \frac{\Lambda_b}{\mu_b H_b(\mu_b + \delta_b)} \left[\frac{\beta_b S_b I_b}{H_b + I_b} - (\mu_b + \delta_b) I_b\right] \\
&= R_{\bar{b}} S_b \frac{I_b}{H_b + I_b} - \frac{\Lambda_b I_b}{\mu_b H_b} \\
&\leq R_{\bar{b}} S_b \frac{I_b}{H_b} - \frac{\Lambda_b I_b}{\mu_b H_b} \\
&\leq R_{\bar{b}} \frac{\Lambda_b I_b}{\mu_b H_b} - \frac{\Lambda_b I_b}{\mu_b H_b} \quad \text{where at the DFE, we have} \\
N_b &\leq \frac{\Lambda_b}{\mu_b} \Rightarrow S_b \leq \frac{\Lambda_b}{\mu_b} \\
&= \frac{\Lambda_b I_b}{\mu_b H_b}\left(R_{\bar{b}} - 1\right) < 0 \text{ if } R_{\bar{b}} < 1.
\end{aligned}$$

Since $\Gamma_b = \left\{(S_b, I_b) \in \mathbb{R}_+^2 : \frac{dL}{dt} = 0\right\} = \left\{(S_b, I_b) \in \mathbb{R}_+^2 : S_b = \frac{\Lambda_b}{\mu_b}, I_b = 0\right\} = \{E_b^0\}$, by LaSalle's invariance principle (Hale, 1969), E_b^0 is globally stable.

Theorem A.2. (Global stability of the DFE for the avian-human HSI model (Chong et al., 2014)). *Given that* $E_{ah}^0 = (S_b^0, I_b^0, S_h^0, I_a^0)$, *the DFE* (E_{ah}^0) *is globally stable in* $\Gamma_{ah} = \{(S_b, I_b, S_h, I_a) \in \mathbb{R}_+^4 : S_b, I_b \leq N_b, S_h, I_a \leq N_h\}$ *if* $R_{ah} < 1$.

Proof. Since the eigenvalues ($\lambda_{\pm}$) of $\mathbf{FV}^{-1}(E^0_{ah})$ are $\lambda_+ = \frac{\beta_b \Lambda_b}{\mu_b H_b(\mu_b+\delta_b)}$ and $\lambda_- = 0$, we only take I_b of the Lyapunov function $L(S_b, I_b, S_h, I_a) = \frac{\Lambda_b}{\mu_b H_b(\mu_b+\delta_b)} I_b$ into consideration. At the DFE, we have $L(S^0_b, I^0_b, S^0_h, I^0_a) = L\left(\frac{\Lambda_b}{\mu_b}, 0, \frac{\Lambda_h}{\mu_h}, 0\right) = 0$, and similarly to what we did in Theorem A.1, E^0_{ah} is globally stable.

Theorem A.3. (Global stability of the DFE for the avian-only isolation model). *Letting* $E^0_T = (S^0_b, I^0_b, T^0_b, R^0_b)$, *the DFE* (E^0_T) *is said to be globally stable in the interior* $\Gamma_T = \{(S_b, I_b, T_b, R_b) \in \mathbb{R}^4_+ : S_b, I_b, T_b, R_b \le N_b\}$ *if* $R_T < 1$.

Proof. We consider a Lyapunov function, $L(S_b, I_b, T_b, R_b) = \frac{\Lambda_b}{\mu_b H_b(\mu_b+\delta_b+\psi_b)} I_b$. At the DFE of isolation model, we have $L(S^0_b, I^0_b, T^0_b, R^0_b) = L\left(\frac{\Lambda_b}{\mu_b}, 0, 0, 0\right) = 0$, and its derivative is

$$
\begin{aligned}
\frac{dL}{dt} &= \frac{\Lambda_b}{\mu_b H_b(\mu_b+\delta_b+\psi_b)} I_b{}' \\
&= \frac{\Lambda_b}{\mu_b H_b(\mu_b+\delta_b+\psi_b)} \left[\frac{\beta_b S_b I_b}{H_b + I_b} - (\mu_b+\delta_b+\psi_b) I_b\right] \\
&= R_T S_b \frac{I_b}{H_b + I_b} - \frac{\Lambda_b I_b}{\mu_b H_b} \\
&\le R_T S_b \frac{I_b}{H_b} - \frac{\Lambda_b I_b}{\mu_b H_b} \\
&\le R_T \frac{\Lambda_b I_b}{\mu_b H_b} - \frac{\Lambda_b I_b}{\mu_b H_b} \quad \text{where at the DFE, we have} \\
N_b &\le \frac{\Lambda_b}{\mu_b} \Rightarrow S_b \le \frac{\Lambda_b}{\mu_b} \\
&= \frac{\Lambda_b I_b}{\mu_b H_b}(R_T - 1) < 0 \text{ if } R_T < 1.
\end{aligned}
$$

As a result, E^0_T is globally stable.

B. List of parameter values

The human inflow (Λ_h), natural death rate of humans (μ_h), rate at which birds contract avian influenza (β_b), and additional disease death rate due to the avian strain in birds (δ_b) were taken into account in the Philippines. While the total human population is represented by $N_h(0)$, the birth rate and the average lifespan of the humans (per year) is 23.7% and 69.2 years, respectively. For β_b and δ_b, the duration of the H5N6 outbreak is estimated at 30 days.

Since the case of bird-to-human transmission and death in humans due to H5N6 were not present in the Philippines, the rate at which humans contract avian influenza from the birds (β_{bh}) and additional disease death rate due to the avian strain in humans (d) in China were considered. With a population estimate of 108 million people in Guangdong of China, the cases of H5N6 infection and death in humans mainly occurred over an estimated period of 912.5 days.

For convenience, the bird inflow (Λ_b), natural death rate of birds (μ_b), and half-saturation constant for birds with avian strain (H_b) and humans with avian strain from infected birds (H_{bh}) were obtained from original value presented in previous mathematical modeling studies.

Table 3
Parameter values.

Parameter	Sample value	References
Λ_b	$\frac{2,060}{365}$ individuals per day	(Chong & Smith, 2015)
Λ_h	$\frac{23.7 N_h(0)}{365,000}$ per day	(The World Factbook)
μ_b	$\frac{1}{2\times 365}$ per day	(Iwami, Takeuchi, & Liu, 2009)
μ_h	$\frac{1}{69.2\times 365}$ per day	(The World Factbook)
β_b	$\frac{45,685}{439,197\times 30}$ per day	(Calculation of Infection Rates; OIE)
β_{bh}	$\frac{16}{(108\times 10^6)\times 912.5}$ per day	(Calculation of Infection Rates; Provinces with the Largest Population; WPRO)
β_v	$\frac{45,685}{2\times 439,197\times 30}$ per day	Assumed

(*continued on next page*)

Table 3 (*continued*)

Parameter	Sample value	References
H_b	180,000 individuals	(Chong et al., 2014)
H_{bh}	120,000 individuals	(Chong et al., 2014)
H_v	850 individuals	Assumed
d	$\frac{6}{(108\times10^6)\times912.5}$ per day	(Cause-specific mortality rate; Provinces with the Largest Population; WPRO)
δ_b	$\frac{45,682}{439,197\times30}$ per day	(Cause-specific mortality rate; OIE)
γ_b	0.003 per day	Assumed
$S_b(0)$	244,956 birds	(OIE)
$I_b(0)$	36,485 birds	(OIE)
$S_h(0)$	171,977 humans	(San Isidro; Jaen; San Luis)
$I_a(0)$	0 humans	(DOH chief)
$V_b(0)$	0 birds	Assumed
$T_b(0)$	0 birds	Assumed
$R_b(0)$	0 birds	(OIE)

Appendix A. Supplementary data

Supplementary data related to this article can be found at https://doi.org/10.1016/j.idm.2018.03.004.

References

Analysis: H5N6 avian influenza strain can easily spread from bird to bird. (2016, November 29). Mainichi Daily News. Retrieved November 07, 2017, from https://mainichi.jp/english/articles/20161129/p2a/00m/0na/015000c.

Avian influenza, including influenza A (H5N1), in humans: WHO interim infection control guidelines for health-care facilities. (n.d.). Retrieved November 7, 2017, from http://www.wpro.who.int/emerging_diseases/documents/docs/AI_Inf_Control_Guide_10May2007.pdf.

Avian flu poultry ban partially lifted | Headlines, News, The Philippine Star | philstar.com. (n.d.). Retrieved November 12, 2017, from http://www.philstar.com/headlines/2017/08/23/1731805/avian-flu-poultry-ban-partially-lifted.

Avian Flu: Questions & Answers. (n.d.). Retrieved November 24, 2017, from http://www.fao.org/avianflu/en/qanda.html#top.

Bourne, M.. (n.d.). 7. Graphs on Logarithmic and Semi-Logarithmic Axes. Retrieved December 11, 2017, from https://www.intmath.com/exponential-logarithmic-functions/7-graphs-log-semilog.php.

Bowman, C., Gumel, A. B., van den Driessche, P., Wu, J., & Zhu, H. (2005). A mathematical model for assessing control strategies against West Nile virus. *Bulletin of Mathematical Biology, 67*(5), 11071133. https://doi.org/10.1016/j.bulm.2005.01.002.

Brauer, F., & Castillo-Chavez, C. (2012). *Mathematical models for communicable diseases*. Society for Industrial and Applied Mathematics. https://doi.org/10.1137/1.9781611972429.fm.

Bressan, A.. (n.d.). Math 411-Ordinary Differential Equations. Differential Equations. Retrieved November 28, 2017, from https://www.math.psu.edu/bressan/PSPDF/M411-review2.pdf.

Buonomo, B., & Lacitignola, D. (2008). On the use of the geometric approach to global stability for three dimensional ODE systems: A bilinear case. *Journal of Mathematical Analysis and Applications, 348*(1), 255–266. https://doi.org/10.1016/j.jmaa.2008.07.021.

Calculation of Infection Rates. (n.d.) Retrieved November 7, 2017, from http://healthcentricadvisors.org/wp-content/uploads/2017/03/Cal_Inf_Rates.pdf.

Castillo-Chavez, C., & Song, B. (2004). Dynamical models of tuberculosis and their applications. *Mathematical Biosciences and Engineering, 1*(2), 361–404. https://doi.org/10.3934/mbe.2004.1.361.

Cause-specific mortality rate | definition of cause-specific mortality rate by Medical dictionary. (n.d.). Retrieved November 12, 2017, from https://medical-dictionary.thefreedictionary.com/cause-specific.mortality.rate.

Chong, N. S., & Smith, R. J. (2015). Modeling avian influenza using Filippov systems to determine culling of infected birds and quarantine. *Nonlinear Analysis: Real World Applications, 24*, 196218. https://doi.org/10.1016/j.nonrwa.2015.02.007.

Chong, N. S., Tchuenche, J. M., & Smith, R. J. (2014). A mathematical model of avian influenza with half-saturated incidence. *Theory in Biosciences, 133*(1), 2338. http://doi.org/10.1007/s12064-013-0183-6.

Claes, F., & Von Dobschuetz, S. (2014). Avian influenza A(H5N6): The latest addition to emerging zoonotic avian influenza threats in east and southeast Asia. *Empres Watch, 30*.

Diekmann, O., Heesterbeek, J. A. P., & Metz, J. A. (1990). On the definition and the computation of the basic reproduction ratio R_0 in models for infectious diseases in heterogeneous populations. *Journal of Mathematical Biology, 28*(4), 365–382. https://doi.org/10.1007/BF00178324.

DOH chief: No human infection of bird flu in PHL so far | News | GMA News Online. (n.d.). Retrieved November 12, 2017, from http://www.gmanetwork.com/news/news/nation/624339/doh-chief-no-human-infection-of-bird-flu-in-phl-so-far/story/.

Gao, S., Chen, L., Nieto, J. J., & Torres, A. (2006). Analysis of a delayed epidemic model with pulse vaccination and saturation incidence. *Vaccine, 24*(35), 6037–6045. https://doi.org/10.1016/j.vaccine.2006.05.018.

Gumel, A. B. (2009). Global dynamics of a two-strain avian influenza model. *International Journal of Computer Mathematics, 86*(1), 85–108. https://doi.org/10.1080/00207160701769625.

Hale, J. K. (1969). *Ordinary differential equations*. New York: Wiley.

Hospital Influenza Working Group. (2009). Management of novel influenza epidemics in Singapore: Consensus recommendations from the hospital influenza (Singapore). *Singapore Medical Journal, 50*, 567–580.

HPAI A. (2015, June 02). *H5 virus background and clinical illness | Avian influenza (Flu)*. Retrieved November 07, 2017, from https://www.cdc.gov/flu/avianflu/hpai/hpai-background-clinical-illness.htm.

Iwami, S., Takeuchi, Y., & Liu, X. (2009). Avian flu pandemic: Can we prevent it? *Journal of Theoretical Biology, 257*(1), 181–190. https://doi.org/10.1016/j.jtbi.2008.11.011.

Jaen, Nueva Ecija - HowlingPixel. (n.d.). Retrieved November 12, 2017, from https://howlingpixel.com/wiki/Jaen,_Nueva_Ecija.

Jones, J. H. (2017, May 1). *Notes On R_0*. Retrieved November 7, 2017, from https://web.stanford.edu/jhj1/teachingdocs/Jones-on-R0.pdf.

Joob, B., & Viroj, W. (2015). H5N6 influenza virus infection, the newest influenza. *Asian Pacific Journal of Tropical Biomedicine, 5*(6), 434–437. https://doi.org/10.1016/j.apjtb.2015.03.001.

Katz, J., Tumpey, T., & Swayne, D. E.. (n.d.). Possible Modes of Transmission of Avian Viruses to People: Studies in Experimental Models (pp. 16). Retrieved November 7, 2017, from http://www.fao.org/docs/eims/upload/250678/aj155e00.pdf.

Korea Freezes Poultry Shipments — Precision Vaccinations. (n.d.). Retrieved November 12, 2017, from http://www.precisionvaccinations.com/highly-pathogenic-h5n6-cases-reach-six-friday.

Liu, Z., & Fang, C. T. (2015). A modeling study of human infections with avian influenza A H7N9 virus in mainland China. *International Journal of Infectious Diseases, 41*, 73–78. https://doi.org/10.1016/j.ijid.2015.11.003.

Liu, S., Pang, L., Ruan, S., & Zhang, X. (2015). Global dynamics of avian influenza epidemic models with psychological effect. *Computational and Mathematical Methods in Medicine, 2015*. https://doi.org/10.1155/2015/913726.

Liu, S., Ruan, S., & Zhang, X. (2015). On avian influenza epidemic models with time delay. *Theory in Biosciences, 134*(3–4), 75–82. https://doi.org/10.1007/s12064-015-0212-8.

Liu, S., Ruan, S., & Zhang, X. (2017). Nonlinear dynamics of avian influenza epidemic models. *Mathematical Biosciences, 283*, 118–135. https://doi.org/10.1016/j.mbs.2016.11.014.

Negative for H5N1: Govt monitoring possible human infections amid Pampanga bird flu. (n.d.). Retrieved November 12, 2017, from http://www.gmanetwork.com/news/news/nation/621553/gov-t-monitoring-possible-human-infections-amid-pampanga-bird-flu/story/.

2017: OIE - World Organisation for Animal Health. (n.d.). Retrieved November 07, 2017, from http://www.oie.int/animal-health-in-the-world/update-on-avian-influenza/.

2016 Provinces with the Largest Population: Guangdong Takes Crown. (n.d.). Retrieved November 07, 2017, from http://www.echinacities.com/news/2016-Provinces-with-the-Largest-Population-Guangdong-Takes-Crown.

San Isidro, Nueva Ecija, Philippines - Universal Stewardship. (n.d.). Retrieved November 12, 2017, from https://www.zamboanga.com/z/index.php?title=San_Isidro%2C_Nueva_Ecija%2C_Philippines.

San Luis, Pampanga - HowlingPixel. (n.d.). Retrieved November 12, 2017, from https://howlingpixel.com/wiki/San_Luis,_Pampanga.

The World Factbook — Central Intelligence Agency. (n.d.). Retrieved November 12, 2017, from https://www.cia.gov/library/publications/the-world-factbook/geos/rp.html.

Van den Driessche, P., & Watmough, J. (2002). Reproduction numbers and sub-threshold endemic equilibria for compartmental models of disease transmission. *Mathematical Biosciences, 180*(1), 29–48. https://doi.org/10.1016/S0025-5564(02)00108-6.

Weisstein, E. W.. (n.d.). Keller-Ressel — from Wolfram MathWorld [Lyapunov Function]. Retrieved November 27, 2017, from http://mathworld.wolfram.com/topics/Keller-Ressel.html.

WHO — Options for the use of human H5N1 influenza vaccines and the WHO H5N1 vaccine stockpile. (n.d.). Retrieved November 07, 2017, from http://www.who.int/csr/resources/publications/WHO_HSE_EPR_GIP_2008_1/en/.

World Health Organization. (2017). *Weekly epidemiological record Relevpidmiologique hebdomadaire* (Vol. 92, pp. 453–476). Retrieved from http://www.who.int/wer.

WPRO — Avian Influenza. (n.d.). Retrieved November 12, 2017, from http://www.wpro.who.int/emerging_diseases/AvianInfluenza/en/.

Yang, J., Zhang, F., & Wang, X. (2007, July). A class of SIR epidemic model with saturation incidence and age of infection. In *Software engineering, artificial intelligence, networking, and parallel/distributed computing, 2007. SNPD 2007. Eighth ACIS international conference on* (Vol. 1, pp. 146–149). IEEE.

Zhang, X., Zou, L., Chen, J., Fang, Y., Huang, J., Zhang, J., et al. (2017). Avian influenza A H7N9 virus has been established in China. *Journal of Biological Systems, 25*, 605–623. https://doi.org/10.1142/S0218339017400095.